

An explanation of one loop induced $h \rightarrow \mu\tau$ decay

Seungwon Baek,^{1,*} Takaaki Nomura,^{1,†} and Hiroshi Okada^{2,‡}

¹*School of Physics, KIAS, Seoul 130-722, Korea*

²*Physics Division, National Center for Theoretical Sciences, Hsinchu, Taiwan 300*

(Dated: June 14, 2016)

Abstract

We discuss a possibility to explain the excess of $h \rightarrow \mu\tau$ at one-loop level. We introduce three generation of vector-like lepton doublet L' and two singlet scalars $S_{1,2}$ which are odd under Z_2 , while all the standard model fields are even under this discrete symmetry. We show that S_1 can be a good dark matter candidate. We show that we can explain the dark matter relic abundance, large part of the discrepancy of muon $g - 2$ between experiments and the standard model predictions, as well as the $h \rightarrow \mu\tau$ excess of ~ 1 %, while evading constraints from experiments of dark matter direct detection and charged lepton flavor violating processes. We also consider prospects of production of S_2 at LHC with energy $\sqrt{s} = 14$ TeV.

Keywords:

*Electronic address: swbaek@kias.re.kr

†Electronic address: nomura@kias.re.kr

‡Electronic address: macokada3hiroshi@gmail.com

I. INTRODUCTION

The mechanism of the electroweak symmetry breaking is being further understood by the discovery of the Standard Model(SM)-like Higgs boson with mass around 125 GeV at the ATLAS [1] and CMS [2] experiments. Furthermore, we would obtain some insight on physics beyond the SM by exploring nature of the Higgs boson such as its decay channels and scalar potential.

The CMS [3] and ATLAS [4] collaborations reported the results on their search for rare Higgs decay $h \rightarrow \mu\tau$ with the dataset obtained at the LHC 8 TeV. An excess of the events was observed by CMS, with a significance of 2.4σ , where the best fit value of branching ratio is $BR(h \rightarrow \mu\tau) = (0.84^{+0.39}_{-0.37})\%$. ATLAS' best fit value is $BR(h \rightarrow \mu\tau) = (0.77 \pm 0.62)\%$, consistent with but less significant than CMS. Since the lepton flavor violating Higgs decay is highly suppressed in the SM, their findings are an intriguing hint indicating new physics (NP) which induces lepton flavor violation in the charged lepton sector, although we need more data to get conclusive evidence for NP. Actually, inspired by the excess, new physics effects in $h \rightarrow \mu\tau$ decay have been studied in [5–41]. Earlier works on the flavor violating Higgs decay can be found in [42–52].

In this paper, we investigate lepton flavor violating effect which is mediated by an exotic lepton doublet L' and inert singlet scalars S which are odd under discrete symmetry Z_2 . The interaction term $\bar{L}L'S$ allowed by both the SM gauge and the Z_2 symmetries often appears in radiative seesaw models, providing active neutrino masses. The neutral components of L' or S can be also good dark matter(DM) candidates. In addition lepton flavor violating (LFV) Higgs decay can be induced at one-loop level with the interaction. Thus this interaction provides interesting effects connecting active neutrino masses, dark matter, and lepton flavor violating Higgs decays. Focusing on the interaction, we explore $h \rightarrow \mu\tau$, charged lepton flavor violations, anomalous magnetic moment of muon and relic density of bosonic dark matter candidate, considering a specific model as an example. Then we search for the parameter region which explains the excess of $h \rightarrow \mu\tau$ observed by CMS with sizable muon magnetic moment and observed relic density of DM, taking into account the constraints from flavor violating lepton decays. Furthermore we discuss possible signature of our scenario which could be tested at the LHC.

This paper is organized as follows. In Sec. II, we show our model, including LFVs, muon

	Lepton Fields			Scalar Fields	
	L_L	e_R	$L'_{L(R)}$	Φ	S^m
$SU(2)_L$	2	1	2	2	1
$U(1)_Y$	$-\frac{1}{2}$	-1	$-\frac{N}{2}$	$\frac{1}{2}$	$\frac{-1+N}{2}$
Z_2	$+$	$+$	$-$	$+$	$-$

TABLE I: Contents of fermion and scalar fields and their charge assignments under $SU(2)_L \times U(1)_Y$, where $m \equiv \frac{-1+N}{2}$ is the quantum number of the electric charge.

anomalous magnetic moment, and LFV Higgs decay. In Sec. III, we carry out numerical analysis including bosonic DM candidate to explain relic density and direct detection in a specific case. We conclude and discuss in Sec. IV.

II. MODEL SETUP

In this section, we explain our model. The particle contents and their charges are shown in Table I. We add three iso-spin doublet vector-like exotic fermions L' with hypercharge $-N/2$, and an isospin singlet scalar S^m with $(-1+N)/2$ hypercharge to the SM, where they are odd under Z_2 , $N(\geq 1)$ is an odd integer and $m(\equiv \frac{N-1}{2})$ is the electric charge of S . Then we define the exotic lepton as

$$L' \equiv [\Psi^{-m}, \Psi^{-m-1}]^T. \quad (\text{II.1})$$

We assume that only the SM Higgs Φ have vacuum expectation value (VEV), which is symbolized by $v/\sqrt{2}$.

The relevant Lagrangian and Higgs potential under these symmetries are given by

$$\begin{aligned} -\mathcal{L}_Y &= (y_\ell)_{ij} \bar{L}_{Li} \Phi e_{Rj} + (y_L)_{ij} \bar{L}_{Li} L'_{Rj} S^m + (M_L)_{ij} \bar{L}'_{Li} L'_{Rj} + \text{h.c.}, \\ \mathcal{V} &= m_\Phi^2 \Phi^\dagger \Phi + m_S^2 |S^m|^2 + \lambda_\Phi |\Phi^\dagger \Phi|^2 + \lambda_S |S^m|^4 + \lambda_{\Phi S} |\Phi|^2 |S^m|^2 \end{aligned} \quad (\text{II.2})$$

where the first term of \mathcal{L}_Y can generates the SM charged-lepton masses $m_\ell \equiv y_\ell v/\sqrt{2}$ after the spontaneous electroweak symmetry breaking by VEV of Φ . We assume all the coefficients

Process	(b, a)	Experimental bounds (90% CL)
$\mu^- \rightarrow e^- \gamma$	(2, 1)	$\text{Br}(\mu \rightarrow e \gamma) < 5.7 \times 10^{-13}$
$\tau^- \rightarrow e^- \gamma$	(3, 1)	$\text{Br}(\tau \rightarrow e \gamma) < 3.3 \times 10^{-8}$
$\tau^- \rightarrow \mu^- \gamma$	(3, 2)	$\text{Br}(\tau \rightarrow \mu \gamma) < 4.4 \times 10^{-8}$

TABLE II: Summary of $\ell_b \rightarrow \ell_a \gamma$ process and the lower bound of experimental data [54].

are real and positive for simplicity. The scalar fields can be parameterized as

$$\Phi = \begin{bmatrix} w^+ \\ \frac{v+h+iz}{\sqrt{2}} \end{bmatrix}, \quad (\text{II.3})$$

where $v \simeq 246$ GeV is VEV of the Higgs doublet, and w^\pm and z are Goldstone bosons which are absorbed by the longitudinal component of W and Z boson, respectively. Inserting the tadpole condition; $\partial \mathcal{V} / \partial \phi|_v = 0$, the SM Higgs mass is given by $\sqrt{2\lambda_\Phi} v$. The mass eigenstate S'^m of the exotic scalar has mass

$$m_{S'} = m_S^2 + \frac{\lambda_\Phi S v^2}{2}. \quad (\text{II.4})$$

A. Lepton Flavor Violations and Muon anomalous magnetic moment

First, let us consider the LFV decays in the charged lepton sector, which impose constraints on the $h \rightarrow \mu \tau$ anomaly. They are summarized in Table II. The processes $\ell_b \rightarrow \ell_a \gamma$ ($b > a$) arise from one-loop diagrams through the term $(y_L)_{ij} (\bar{\ell}_L)_i (\Psi^{-m-1})_j S^m$. Then their branching ratios $\text{BR}(\ell_b \rightarrow \ell_a \gamma)$ are defined by

$$\text{BR}(\ell_b \rightarrow \ell_a \gamma) = \frac{48\pi^3 \alpha_{\text{em}} C_b}{G_F^2 m_b^2} (|(a_R)_{ab}|^2 + |(a_L)_{ab}|^2), \quad (\text{II.5})$$

where α_{em} is the fine structure constant, $C_b \approx (1, 1/5)$ for $(b = \mu, \tau)$, $G_F \approx 1.17 \times 10^{-5}$ GeV⁻² is the Fermi constant. The Wilson coefficients $(a_R)_{ab}$ are obtained to be

$$(a_R)_{ab} = -\frac{m_b}{(4\pi)^2} \sum_{i=1}^3 (y_L^\dagger)_{ai} (y_L)_{ib} [(m+1)F[m_{S^m}, M_{\Psi^{m+1}}] + mF[M_{\Psi^{m+1}}, m_{S^m}]], \quad (\text{II.6})$$

$$F[m_a, m_b] \equiv \frac{2m_a^6 + 3m_a^4 m_b^2 + 12m_a^4 m_b^2 \ln \left[\frac{m_b}{m_a} \right] - 6m_a^2 m_b^4 + m_b^6}{12(m_a^2 - m_b^2)^4}, \quad (\text{II.7})$$

while the chirality-flipped ones are suppressed by small mass ratios: $a_L = a_R m_a / m_b$. Here $M_{\Psi^{1+m}} (= M_{\Psi^m}) = M_L$.

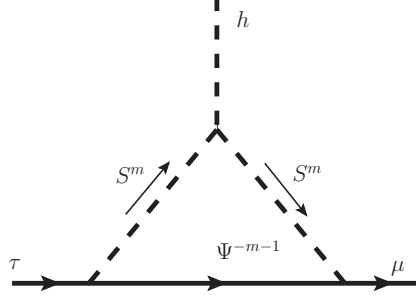


FIG. 1: One-loop Feynman diagram for $h \rightarrow \mu\tau$. The Higgs (h) line can also be attached to external μ or τ lines.

Our formula of the muon anomalous magnetic moment (muon $g-2$) is also given in terms of $a_{L/R}$ by

$$\Delta a_\mu \approx -m_\mu(a_R)_{22}, \quad (\text{II.8})$$

where the lower index 2 of a_R is muon eigenstate.

B. $h \rightarrow \mu\tau$ excess

In our case, the excess of $h \rightarrow \mu\tau$ can be generated at one-loop level as the leading contribution. Its Feynman diagram is shown in Fig. 1.

The resultant decay rate formulas are expressed as

$$\Gamma(h \rightarrow \mu\tau) = \frac{|\bar{M}|^2}{8\pi m_h^2} \sqrt{\frac{(m_h + m_\mu)^2 - m_\tau^2}{2m_h} \frac{(m_h - m_\mu)^2 - m_\tau^2}{2m_h}}, \quad (\text{II.9})$$

$$|\bar{M}|^2 = \sum_{i=1}^3 \frac{|(y_L^\dagger)_{2i}(y_L)_{i3}\mu_{hSS}|^2}{(4\pi)^4} [(m_h^2 - m_\mu^2 - m_\tau^2)(m_\mu^2 F_L^2 + m_\tau^2 F_R^2) - 4m_\mu^2 m_\tau^2 F_L F_R], \quad (\text{II.10})$$

$$F_L = \int \frac{\delta(x+y+z-1)y^2 dx dy dz}{(z^2 - z)m_\mu^2 + (x^2 - y)m_\tau^2 - xz(m_h^2 - m_\mu^2 - m_\tau^2) + xM_{\Psi^{m+1}}^2 + (y+z)m_{S^m}^2}, \quad (\text{II.11})$$

$$F_R = \int \frac{\delta(x+y+z-1)z^2 dx dy dz}{(z^2 - z)m_\mu^2 + (x^2 - y)m_\tau^2 - xz(m_h^2 - m_\mu^2 - m_\tau^2) + xM_{\Psi^{m+1}}^2 + (y+z)m_{S^m}^2}, \quad (\text{II.12})$$

where $\mu_{hSS} \equiv \lambda_{\Phi S} v/2$ is the strength of the trilinear $hS^{\pm m}S^{\mp m}$ interaction. Then the branching ratio reads

$$\text{BR}(h \rightarrow \mu\tau) \approx \frac{\Gamma(h \rightarrow \mu\tau)}{\Gamma(h \rightarrow \mu\tau) + \Gamma(h)}, \quad (\text{II.13})$$

where $\Gamma(h) \approx 4.2 \times 10^{-3}$ GeV is the total decay width of the SM Higgs boson at 125.5 GeV.

III. THE CASE $m = 0$

Let us first consider briefly the case $m \neq 0$ before we discuss more constrained model with $m = 0$. DM candidate does not exist in this case. Nonzero m , however, can enhance the muon $g - 2$ as well as the LFVs. Thus one can obtain the sizable value of muon $g - 2$ which can as large as $\mathcal{O}(10^{-9})$, while one can assume that the Yukawa coupling matrix (y_L) is diagonal or at least one of $m_{S^m}, m_{\Psi^{m+1}}$'s are very large to evade the constraints of LFVs. The model has all the ingredients to generate Majorana neutrino mass matrix via radiative seesaw mechanism, which, however, is not straightforward due to the Dirac nature of L' [53]. In this sense, radiative neutrino models with (at least) two-loop diagrams are favored for nonzero m . Another difficulty is decays of S^m , which is charged scalar for $m \neq 0$, into the SM fields is not possible. Some more additional fields need to be introduced in order to evade this problem for each m , and the detailed phenomenology depends on the implemented models. Thus we do not discuss the case of nonzero m further.

We will focus on the special case of $m = 0$ because it includes a DM candidate $S^m \equiv S^0$ in the boson sector, which can possibly solve the above mentioned problems of $m \neq 0$ case. Notice here that the neutral component of the $SU(2)_L$ -doublet L' fermion cannot be DM due to the interaction with the SM neutral gauge boson Z that is ruled out by the direct detection search.

We redefine the exotic fields as ($S^0 \equiv$) $S = (S_R + iS_I)/\sqrt{2}$, $L' \equiv [N, E]^T$. The Lagrangian in (III.23) can be rewritten as

$$-\mathcal{L}_Y = (y_\ell)_{ij} \bar{L}_{Li} \Phi e_{Rj} + (y_L)_{ij} \bar{L}_{Li} L'_{Rj} S + (M_L)_{ij} \bar{L}'_{Li} L'_{Rj} + \text{h.c.}, \quad (\text{III.1})$$

$$\begin{aligned} \mathcal{V} = & m_\Phi^2 \Phi^\dagger \Phi + (m_{S_1}^2 S^2 + \text{h.c.}) + m_{S_2}^2 |S|^2 + \lambda_\Phi |\Phi^\dagger \Phi|^2 \\ & + \sum_{i=0}^4 [\lambda_i S_i (S^*)^{4-i} + \text{h.c.}] + (\lambda_{\Phi S_1} |\Phi|^2 S^2 + \text{h.c.}) + \lambda_{\Phi S_2} |\Phi|^2 |S|^2, \end{aligned} \quad (\text{III.2})$$

where the corresponding trilinear coupling $\mu_{hS^\pm m_{S^\mp m}}$ appearing on Eq. (II.12) is rewritten by $\mu_{hS_R S_R} \equiv (\lambda_{\Phi S_1} + \frac{\lambda_{\Phi S_2}}{2})v$ and $\mu_{hS_I S_I} \equiv (-\lambda_{\Phi S_1} + \frac{\lambda_{\Phi S_2}}{2})v$. The formulae for LFVs, muon $g - 2$, and the excess of $h \rightarrow \mu\tau$ are obtained simply by putting $m = 0$ in Eqs. (II.7), (II.8), and (II.12). Now we discuss the property of a DM candidate $S_{R/I}$ in the next subsection.

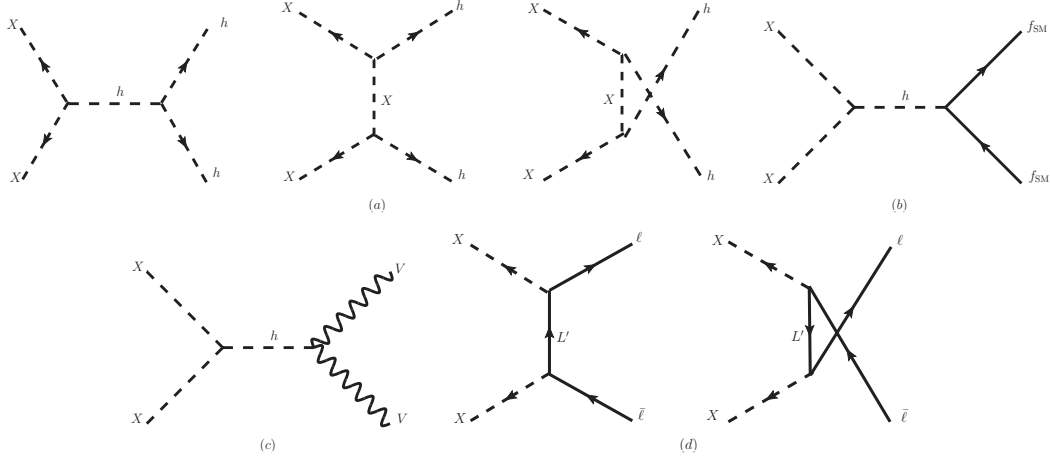


FIG. 2: Feynman diagrams for the DM annihilations.

A. Dark Matter Candidate

Before the analysis of the DM candidate let us make some assumptions for simplicity as follows: $X(=S) \equiv S_R$ or S_I ($M_X \equiv m_{S_R} \approx m_{S_I}$), $\mu_{hSS} \equiv \mu_{hS_R S_R} \approx \mu_{hS_I S_I} \approx \frac{\lambda_{\Phi S_2} v}{2}$, therefore $\lambda_{\Phi S_1} \ll \lambda_{\Phi S_2}$.

Relic density: The thermal averaged annihilation cross section comes from the processes $2X \rightarrow 2h$, $2X \rightarrow f_{SM} \bar{f}_{SM}$, $2X \rightarrow V V^{(*)}$, and L' -exchanging $2X \rightarrow \ell \bar{\ell} (\nu_L \bar{\nu}_L)$ [55, 56], f_{SM} and V being the SM fermions and gauge bosons, respectively. The Feynman diagrams are shown in Fig. 2. It can be calculated as

$$\sigma v_{\text{rel}} \approx \sum_{f=h, f_{SM}, \ell, V} \int_0^\pi \sin \theta d\theta \frac{|\bar{M}|^2}{16\pi s} \sqrt{1 - \frac{4m_f^2}{s}}, \quad (\text{III.3})$$

where

$$|\bar{M}|^2 \approx |\bar{M}(2X \rightarrow 2h)|^2 + \sum_{f_{SM}=(t,b)} |\bar{M}(2X \rightarrow f_{SM}\bar{f}_{SM})|^2 + \sum_{\ell=(\ell,\nu_L)} |\bar{M}(2X \rightarrow \ell\bar{\ell})|^2 + \sum_{V=(Z,W^\pm)} |\bar{M}(2X \rightarrow VV^*)|^2, \quad (\text{III.4})$$

$$|\bar{M}(2X \rightarrow 2h)|^2 \approx \lambda_{\Phi S_2}^2 \left| 1 + \frac{3v^2\lambda_\Phi}{2(s-m_h^2)} + \frac{v^2}{4} \left[\frac{1}{t-M_X^2} + \frac{1}{u-M_X^2} \right] \right|^2, \quad (\text{III.5})$$

$$|\bar{M}(2X \rightarrow f_{SM}\bar{f}_{SM})|^2 \approx \frac{48\mu_{hSS}^2 m_{f_{SM}}^2}{(s-m_h^2)^2 v^2} \left(\frac{s}{2} - 2m_{f_{SM}}^2 \right), \quad (\text{III.6})$$

$$|\bar{M}(2X \rightarrow VV^*)|^2 \approx \frac{4\lambda_{\Phi S_2}\mu_{hSS}^2 m_V^4}{(s-m_h^2)^2 v^2} \left(2 + \frac{(s/2 - m_V^2)^2}{m_V^4} \right), \quad (\text{III.7})$$

$$|\bar{M}(2X \rightarrow \ell\bar{\ell})|^2 \approx 8 \sum_{a,b}^{2-3} \sum_{i=1-3} |(y_L)_{i,b}|^2 |(y_L)_{i,a}|^2 \times \left[4 \left(\frac{p_1 \cdot k_1}{t} + \frac{p_2 \cdot k_1}{u} \right) \left(\frac{p_1 \cdot k_2}{t} + \frac{p_2 \cdot k_2}{u} \right) - sM_X^2 \left(\frac{1}{t^2} + \frac{1}{u^2} \right) - 2s \left(\frac{p_1 \cdot p_2}{tu} \right) \right], \quad (\text{III.8})$$

where s, t, u are the Mandelstam variables; $p_1, p_2(k_1, k_2)$ are four-momenta of the initial (final) states; $\lambda_{\Phi S_2} = 2\mu_{hSS}/v$; among all the SM fermions in f_{SM} heavy quarks such as top quark or bottom quark dominate; $V(=Z, W^\pm)$ is the SM vector gauge bosons. We neglect the masses of the SM leptons (ν_L, ℓ) in the final states. Notice here that the mode $2X \rightarrow \ell\bar{\ell}$ is d -wave dominant. To include its effect we retain terms up to the v_{rel}^4 in v_{rel} expansion for all the modes. Then the relic density of DM is finally obtained from

$$\Omega h^2 \approx \frac{1.07 \times 10^9}{g_*^{1/2} M_{\text{pl}} [\text{GeV}] \int_{x_f}^{\infty} \left(\frac{a_{\text{eff}}}{x^2} + 6 \frac{b_{\text{eff}}}{x^3} + 60 \frac{d_{\text{eff}}}{x^4} \right)}, \quad (\text{III.9})$$

where $g_* \approx 100$ is the total number of effective relativistic degrees of freedom at the time of freeze-out, $M_{\text{pl}} = 1.22 \times 10^{19} [\text{GeV}]$ is the Planck mass, $x_f \approx 25$, and a_{eff} , b_{eff} and d_{eff} are coefficients in the v_{rel}^2 expansion of the annihilation cross section:

$$\sigma v_{\text{rel}} \approx a_{\text{eff}} + b_{\text{eff}} v_{\text{rel}}^2 + d_{\text{eff}} v_{\text{rel}}^4. \quad (\text{III.10})$$

The observed relic density reported by Planck suggest that $\Omega h^2 \approx 0.12$ [57]. In terms of the model parameters the expansion coefficients are

$$\begin{aligned}
a_{\text{eff}} \approx & \frac{3\mu_{hSS}^2 \sum_{f=b,t} m_f^2 (M_X^2 - m_f^2)}{2\pi M_X^2 v^2 (m_h^2 - 4M_X^2)^2} \sqrt{1 - \frac{m_f^2}{M_X^2}} \\
& + \frac{\lambda_{\Phi S}^2}{256\pi M_X^2} \left| 2 + v^2 \left(\frac{1}{m_h^2 - 2M_X^2} - \frac{3\lambda_\Phi}{m_h^2 - 4M_X^2} \right) \right|^2 \sqrt{1 - \frac{m_h^2}{M_X^2}} \\
& + \frac{3\mu_{hSS}^2 \sum_{V=W,Z}}{16\pi M_X^2 v^2 (m_h^2 - 4M_X^2)^2} (2m_V^4 + (2M_X^2 - m_V^2)^2) \sqrt{1 - \frac{m_V^2}{M_X^2}}, \tag{III.11}
\end{aligned}$$

where we would not show the explicit forms of b_{eff} and d_{eff} , because they are too complicated.

Direct detection: The DM-nucleon scattering is induced by the SM Higgs exchanging process in our model, which is calculated in non-relativistic limit. The dominant tree-level diagram is obtained by crossing Fig. 2 (b) which gives (III.6). However, the leptons in f_{SM} in the crossed diagram does not contribute to the direct detection process because there is no valence leptons inside nucleons. Although heavy quark contributions to the parton distribution function of nucleon are suppressed, they can make contribution via Higgs-gluon-gluon triangle diagram. Here we estimate the DM-nucleon scattering cross section following Ref. [58]. Firstly we obtain the following effective Lagrangian by integrating out h for non-relativistic momentum transfer,

$$\mathcal{L}_{\text{eff}} = \sum_q \frac{C_{hSS} m_q}{m_h^2} X^2 \bar{q} q, \tag{III.12}$$

where q and m_q represent the corresponding quark fields and the quark masses respectively, the sum is over all quark flavors, and we neglected higher dimensional operators. The coefficient C_{hSS} determines the effective interaction between the quarks and X . The corresponding value in our model is

$$C_{hSS} = \frac{\mu_{hSS}}{v}. \tag{III.13}$$

Then the effective X -nucleon (N) interaction can be written down by

$$\mathcal{L}_{\text{eff}}^N = \frac{f_N C_{hSS} m_N}{m_h^2} X^2 \bar{N} N \tag{III.14}$$

where the effective coupling constant f_N is given by

$$f_N = \sum_q f_q^N = \sum_q \frac{m_q}{m_N} \langle N | \bar{q} q | N \rangle. \tag{III.15}$$

Note that the quark mass m_q is absorbed into the definition of quark mass fraction

$$f_q^N \equiv \frac{m_q}{m_N} \langle N | \bar{q}q | N \rangle. \quad (\text{III.16})$$

The heavy quark contributions are replaced by the gluon contributions by calculating the triangle diagram

$$\sum_{q=c,b,t} f_q^N = \frac{1}{m_N} \sum_{q=c,b,t} \langle N | \left(-\frac{\alpha_s}{12\pi} m_q G_{\mu\nu}^a G^{a\mu\nu} \right) | N \rangle. \quad (\text{III.17})$$

From the scale anomaly, the trace of the stress energy tensor is written as [59]

$$\theta_\mu^\mu = m_N \bar{N}N = \sum_q m_q \bar{q}q - \frac{7\alpha_s}{8\pi} G_{\mu\nu}^a G^{a\mu\nu}. \quad (\text{III.18})$$

From (III.17) and (III.18) we finally obtain

$$\sum_{q=c,b,t} f_q^N = \frac{2}{9} \left(1 - \sum_{q=u,d,s} f_q^N \right), \quad (\text{III.19})$$

which results in

$$f_N = \frac{2}{9} + \frac{7}{9} \sum_{q=u,d,s} f_q^N. \quad (\text{III.20})$$

Here we use the DM-neutron (n) scattering cross section to consider constraints from direct detection where that of DM-proton case is almost same for Higgs portal interaction. Then the spin independent scattering cross section of the X with neutron through the SM Higgs(ϕ) portal process is obtained to be [58]

$$\begin{aligned} \sigma_{\text{SI}}(Xn \rightarrow Xn) \times \left(\frac{\rho_X}{\rho_{DM}} \right) &= \frac{1}{\pi} \frac{\mu_{nX}^2 m_n^2 C_{hSS}^2 f_n^2}{M_X^2 m_h^4} \times \left(\frac{\rho_X}{\rho_{DM}} \right) \simeq \frac{\mu_{hSS}^2 f_n^2}{\pi v^2} \frac{m_n^4}{m_h^4 M_X^2} \left(\frac{\Omega h^2}{0.12} \right) \\ &\approx 5.29 \times 10^{-43} \left(\frac{\mu_{hSS}}{M_X} \right)^2 \left(\frac{\Omega h^2}{0.12} \right) [\text{cm}^2], \end{aligned} \quad (\text{III.21})$$

where m_n is the neutron mass, we approximated $\mu_{nX} = m_n M_X / (m_n + M_X) \simeq m_n$, ρ_X and ρ_{DM} are current density of X and total density of DM, and $f_n \approx 0.287$ (with $f_u^n = 0.0110$, $f_d^n = 0.0273$, $f_s^n = 0.0447$) represents the sum of the contributions of partons to the mass fraction of neutron [60]. The scattering cross section imposes a strong constraint on the parameter space relevant to the DM. The constraint from the LUX experiment is the strongest at present with $\sigma_{\text{SI}} \times \left(\frac{\rho_X}{\rho_{DM}} \right)$ less than $\mathcal{O}(10^{-45}) \text{ cm}^2$ for DM mass about $\mathcal{O}(10)$ GeV [61]. Notice here that the experimental bound on the direct detection is obtained by

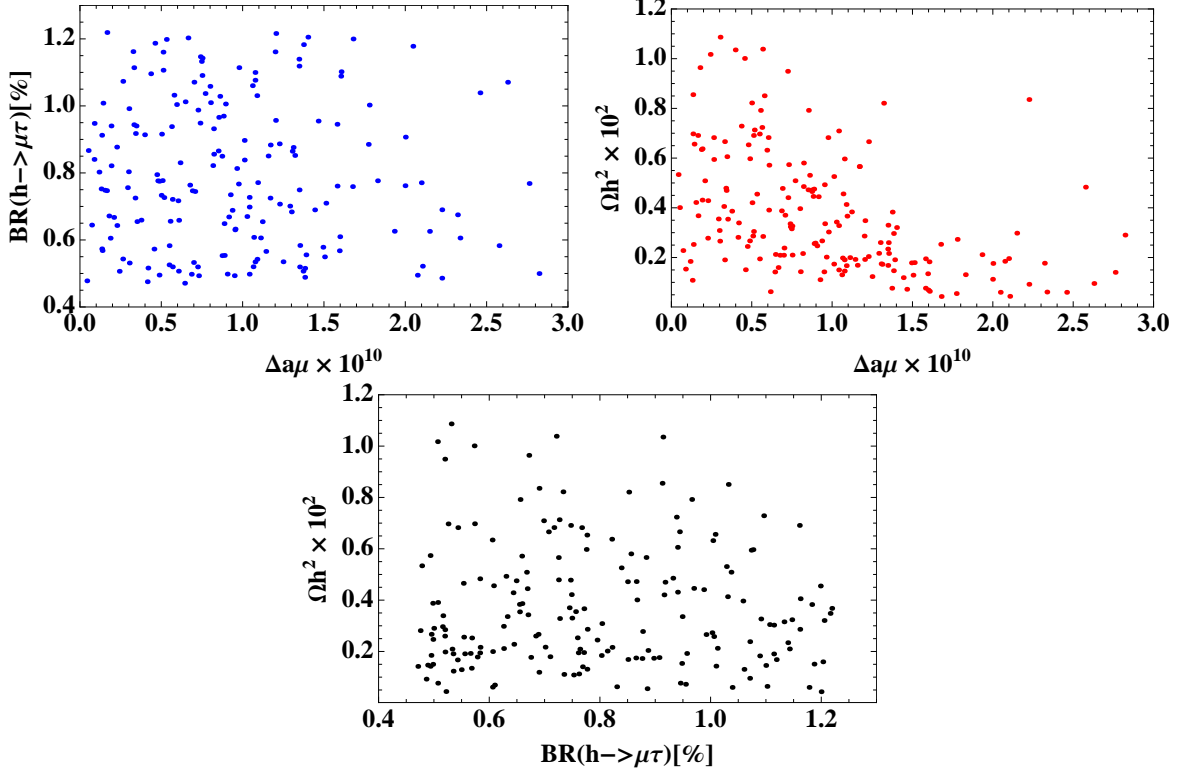


FIG. 3: Numerical results: Each of the top-left, top-right, and bottom figure represents the scattering points in terms of (muon $g - 2$ and the branching ratio of $h \rightarrow \mu\tau$), (relic density and the muon $g - 2$), and (the branching ratio of $h \rightarrow \mu\tau$ and relic density).

assuming that one of the DM components occupies all of the DM components (*i.e.*, $\Omega h^2 = 0.12$) in the current universe. Otherwise we should multiply the factor $\left(\frac{\rho_X}{\rho_{DM}}\right) = \left(\frac{\Omega h^2}{0.12}\right)$ for the scattering cross section as can be seen in Eq. (III.21). It suggests that the upper bound from direct detection is relaxed when our X is subcomponent of DM, because $1 > \left(\frac{\Omega h^2}{0.12}\right)$.

Numerical analysis: Now that all of the analytical formulae are derived, we perform numerical analysis and explore the allowed region. We scan the parameters in the ranges:

$$\begin{aligned}
 M_X \in [100 \text{ GeV}, 500 \text{ GeV}], \quad \mu_{hSS} \in [50 \text{ GeV}, 500 \text{ GeV}], \quad M_L (= M_{E_i} = M_{N_i}) \in [M_X, 1 \text{ TeV}], \\
 (y_L)_{\ell,m} \in [-0.01, 0.01], \quad (\ell, m) = ((1, 1), (2, 1), (3, 1)), \quad (y_L)_{i,j} \in [-\sqrt{4\pi}, 4\pi], \quad (i, j) \neq (\ell, m),
 \end{aligned}
 \tag{III.22}$$

where $M_X = M_S$ denotes DM mass. The ranges are chosen to satisfy perturbativity of $\lambda_{\Phi S}$, the bound from the charged lepton flavor violation, and also electroweak scale new particles are assumed. The result does not change much even if we enlarge the ranges. Here we

assume Yukawa couplings $(y_L)_{ij}$ are small when it has index corresponding to electron in order to satisfy constraint from $\mu \rightarrow e\gamma$.

We scanned the above regions of parameters randomly to obtain the allowed range of $h \rightarrow \mu\tau$ branching ratio and muon $g - 2$, imposing the constraint from dark matter relic density and direct detection experiments. The results are shown in Fig. 3. As we can see in the figure, we can accommodate the excess observed by CMS. In this case, the maximum value of the muon $g - 2$ is around (3×10^{-10}) , which is smaller than the current discrepancy $\mathcal{O}(10^{-9})$ [62]. The relic density is $\mathcal{O}(0.001 - 0.01)$, which is also smaller than the current measurement 0.12 as can be seen in Fig. 3. It is mainly due to the direct detection bound. In order to obtain enough excess of $h \rightarrow \mu\tau$, one has to increase the value of trilinear coupling μ_{hSS} . On the other hand, the direct detection bound suggests $\frac{\mu_{hSS}}{M_X} \lesssim 0.04$, if $\sigma_{SI} \lesssim 10^{-45} \text{ cm}^2$. To evade the constraint from LUX the DM mass scale should be above 100 TeV, which conflicts with relic density and $h \rightarrow \mu\tau$ excess. This leads to the conclusion that S cannot be main source of the relic DM.

To explain DM relic abundance we extend the model as minimally as possible. One of the minimal extension to solve this issue is to introduce another gauge singlet boson having the same charge with S , which we denote by S_2 . Then all the terms of Eq. (III.2) remain in the same form with only the number of terms doubled. For our convenience let us rename two singlet bosons (S_1, S_2) . Then the Lagrangian is simply obtained by replacing, e.g., $y_L \rightarrow y_L^\alpha (\alpha = 1 - 2)$, $\mu_{hSS} \rightarrow \mu_{hS_i S_j} (i, j = 1 - 2)$, *etc.* Explicitly the new terms include

$$-\mathcal{L}_Y \supset \sum_{\alpha=1,2} \left((y_L^\alpha)_{ij} \bar{L}_{L_i} L'_{R_j} S_\alpha - \sum_{\beta=1,2} \lambda_{\Phi S_\alpha S_\beta} |\Phi|^2 S_\alpha S_\beta + \text{h.c.} \right), \quad (\text{III.23})$$

where $\mu_{hS_\alpha S_\beta} \equiv \lambda_{\Phi S_\alpha S_\beta} v/2$ and we neglect $\mu_{hS_1 S_2}$ for simplicity. We assume $M_{S_2} > M_{S_1}$ so that S_1 still remains as a DM candidate. In this case, $\mu_{hS_2 S_2}$ can play a crucial role in generating the excess $h \rightarrow \mu\tau$, while it need not contribute to the interaction of the direct detection searches. We take the same regions given Eq. (III.22) as our new input parameters except the following,

$$M_{S_2} \in \left[\frac{11}{10} \text{ GeV}, 1 \text{ TeV} \right], \quad \mu_{hS_1 S_1} \in [0.01 \text{ GeV}, 0.1 \text{ GeV}], \quad (\text{III.24})$$

and $M_X = M_{S_1}$ in this case. We show the results in Fig. 4, in which relic density is within the current observational value. The maximum value of the muon $g - 2$ is around 1.5×10^{-9} , which can explain the discrepancy $\Delta a_\mu = (26.1 \pm 8.0) \times 10^{-10}$ [63] at the 2σ level. To

obtain $O(10^{-9})$ muon $g-2$, $M_X \in [100 \text{ GeV}, 170 \text{ GeV}]$ and $\mu_{hS_2S_2} \in [20 \text{ GeV}, 150 \text{ GeV}]$ are preferred. For simplicity we assume the mass difference ratio $(M_{S_2} - M_X)/M_X \gtrsim 10\%$ to evade the coannihilation regime. The trilinear coupling $\mu_{hS_1S_1}$ can be decreased by three orders magnitude below the original value of one S model to satisfy the direct detection experiments without affecting other observables, $h \rightarrow \mu\tau$, $(g-2)_\mu$, DM relic density. In this case the DM relic density is achieved dominantly by $2X \rightarrow \ell\bar{\ell}$ channel. Here we provide the typical parameter set as follows:

$$\begin{aligned}
M_X &\approx 146 \text{ GeV}, \quad M_L(= M_{E_i} = M_{N_i}) \approx (663, 980, 460) [\text{TeV}], \\
M_{S_2} &\approx 332 [\text{TeV}], \quad \mu_{hS_1S_1} \approx 0.079 [\text{GeV}], \quad \mu_{hS_2S_2} \approx 23 [\text{GeV}], \\
(y_L)_{\ell,m} &\approx \begin{bmatrix} -0.0076 & -1.0 & 0.16 \\ -0.0076 & -0.83 & -2.8 \\ -0.0063 & 0.38 & -2.4 \end{bmatrix}, \quad (y_L)_{i,j} \approx \begin{bmatrix} -0.0060 & -0.89 & -3.0 \\ -0.0062 & -0.25 & -3.3 \\ 0.0 & 2.5 & -0.38 \end{bmatrix}, \quad (\text{III.25})
\end{aligned}$$

then we can obtain the following observables:

$$\begin{aligned}
(g-2)_\mu &\approx 1.8 \times 10^{-10}, \quad \Omega h^2 \approx 0.12, \quad \text{BR}(h \rightarrow \mu\tau) \approx 0.48\%, \quad \sigma_{\text{SI}} \approx 4.4 \approx 10^{-50} [\text{cm}^2], \\
\text{BR}(\mu \rightarrow e\gamma) &\approx 2.5 \times 10^{-13}, \quad \text{BR}(\tau \rightarrow e\gamma) \approx 8.6 \times 10^{-12}, \quad \text{BR}(\mu \rightarrow \mu\gamma) \approx 1.3 \times 10^{-8}.
\end{aligned} \quad (\text{III.26})$$

Collider phenomenology of our scenario: Now we discuss the signature of our scenario at the LHC. Here we focus on the interaction $\mu_{hS_2S_2} h |S_2|^2$ to produce S_2 via gluon fusion, $gg \rightarrow h \rightarrow S_2 S_2$, since the coupling constant of the interaction hS_2S_2 is required to be large as $O(100)$ GeV in obtaining sizable $h \rightarrow \mu\tau$ branching ratio. The produced S_2 mainly decays into $S_1 h$ through the interaction like vhS_1S_2 in scalar potential where we assume L' is heavier than S_2 for simplicity. It suggests that the S_2 can be measured at the LHC where the signature will be two SM Higgs boson with missing transverse energy. Then the production cross section is numerically estimated with CalcHEP [64] using CTEQ6L PDF [65] by implementing relevant interactions in the code. In Fig. 5, we show the production cross section of $pp \rightarrow S_2 S_2$ as a function of S_2 mass adopting some values of $\mu_{hS_2S_2}$ and collision energy of $\sqrt{s} = 14$ TeV. Here the cross section is at the leading order and it will be larger when we consider K-factor. We find that the cross section can be sizable when $\mu_{hS_2S_2}$ is large and m_{S_2} is around 100 GeV. Note that the cross section becomes significantly large

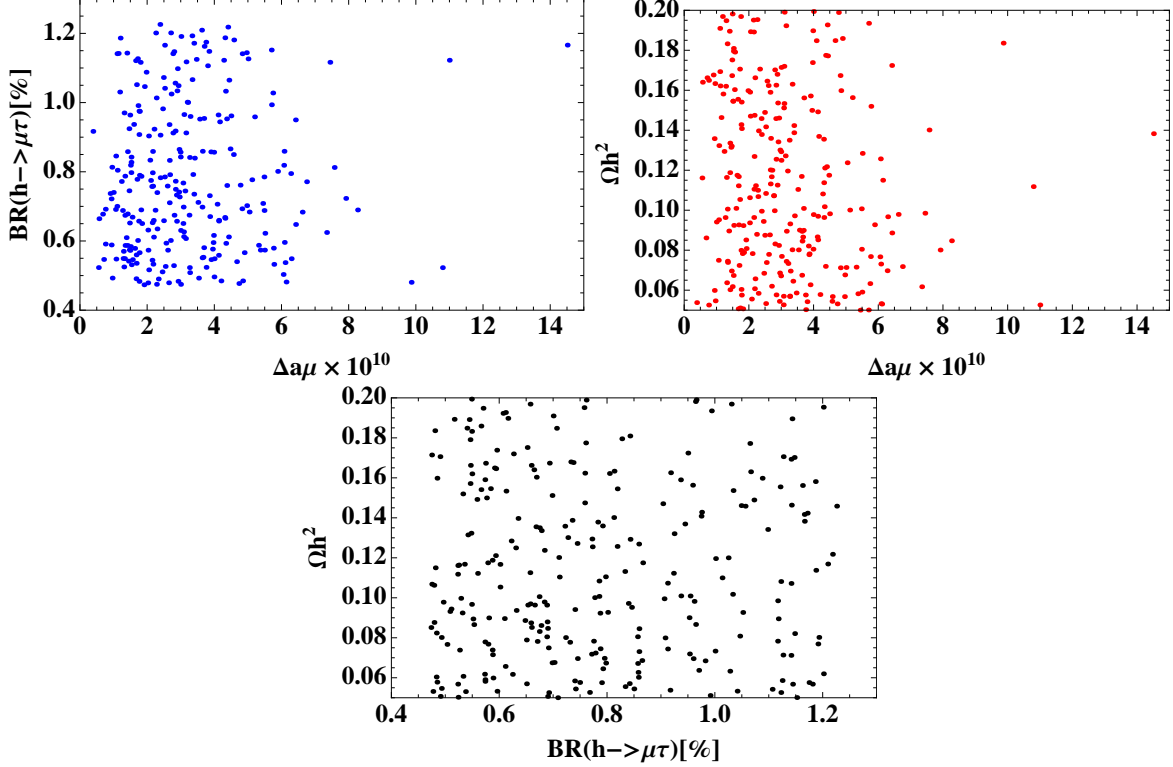


FIG. 4: Numerical results: Each of the top-left, top-right, and bottom figure represents the scattering points in terms of (muon $g - 2$ and the branching ratio of $h \rightarrow \mu\tau$), (relic density and the muon $g - 2$), and (the branching ratio of $h \rightarrow \mu\tau$ and relic density).

when the m_{S_2} close to $m_h/2$ due to resonant enhancement since the process is SM Higgs boson exchanging s-channel, although the resonant point is below our parameter region. Thus some parameter space of our scenario can be tested by exploring $hh\not{E}_T$ signal at the LHC. In Table III, we also show the number of expected events at the LHC 14 TeV for several values of m_{S_2} and $\mu_{hS_2S_2}$ with luminosity of 100 fb^{-1} as a reference. Moreover the study of exotic lepton production will be also interesting. The detailed simulation study is beyond the scope of this paper and it is left as future study.

IV. CONCLUSIONS AND DISCUSSIONS

We studied a possibility to explain the excess of $h \rightarrow \mu\tau$ and muon $g - 2$ in a model with a dark matter candidate. At first, we provided a simple set up with generic hypercharge

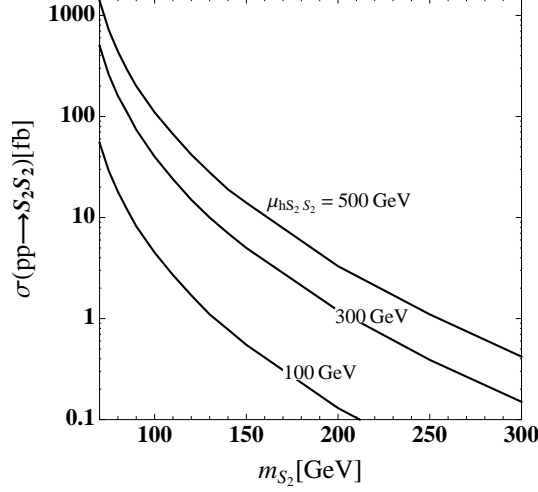


FIG. 5: The production cross section for $pp \rightarrow S_2 S_2$ as a function of m_{S_2} with collision energy of $\sqrt{s} = 14$ TeV.

	$m_{S_2} = 100$ GeV	$m_{S_2} = 200$ GeV	$m_{S_2} = 300$ GeV
$\mu_{hS_2S_2} = 100$ GeV	4.5×10^2	13.	1.7
$\mu_{hS_2S_2} = 200$ GeV	4.0×10^3	1.2×10^2	15.
$\mu_{hS_2S_2} = 300$ GeV	1.1×10^4	3.3×10^2	42.

TABLE III: Number of expected $hh\cancel{E}_T$ events at the LHC 14 TeV for several values of m_{S_2} and $\mu_{hS_2S_2}$ with luminosity of 100 fb^{-1} .

assignments, in which we formulated the lepton flavor violations, muon $g - 2$, and the branching ratio of $h \rightarrow \mu\tau$. Then we moved on to the specific case where single DM candidate can be included. We found the sizable excess of $h \rightarrow \mu\tau$ has been obtained. However the relic density and muon $g - 2$ cannot be explained due to the stringent constraint from the direct detection via Higgs portal.

We extended the model as minimally as possible so that we can explain the relic density and the muon $g - 2$ as well as $h \rightarrow \mu\tau$. We introduced another gauge singlet boson S_2 having the same quantum numbers with S_1 , and we solved all the issues. At the end, we have discussed the signature of our scenario at the LHC, focusing on the interaction $\mu_{hS_2S_2} h |S_2|^2$ to produce S_2 via gluon fusion, $gg \rightarrow h \rightarrow S_2 S_2$. This is because the coupling constant of the interaction hS_2S_2 is required to be large as $O(100)$ GeV in obtaining sizable $h \rightarrow \mu\tau$ branching ratio. The produced S_2 mainly decays into $S_1 h$ through the coupling

vhS_1S_2 in scalar potential. It suggests that the S_2 can be searched for at the LHC where the signature is two SM Higgs boson with missing transverse energy. We found that the cross section can be sizable when m_{S_2} is around 100 GeV for $\sqrt{s} = 14$ TeV pp collision.

It is worth to mention possible application of our model to the other sectors such as neutrinos. Since our set up is very simple, several applications to the neutrino sector could be possible. Let us just briefly comment on two possibilities. First, if we introduce a gauge singlet Majorana fermion with Z_2 odd charge, we can explain the neutrino masses and mixings at the one-loop level, and the fermion can be a good DM candidate. Second possibility is to introduce a $SU(2)$ triplet boson with nonzero VEV. In this case, the neutrino masses and the mixings are induced through the type-II seesaw mechanism. The neutral component of the $SU(2)_L$ doublet exotic lepton can be a DM candidate since sizable mass splitting between right-handed and left handed neutral fermions can be obtained to evade the strong bound from direct detection experiments [66]. However since there is no new source of the muon $g - 2$ for both cases, we need some extensions such as we have mainly discussed in our paper.

Acknowledgments

H. O. is sincerely grateful for all the KIAS members, Korean cordial persons, foods, culture, weather, and all the other things. This work is supported in part by National Research Foundation of Korea (NRF) Research Grant NRF-2015R1A2A1A05001869 (SB).

-
- [1] S. Chatrchyan *et al.* [CMS Collaboration], Phys. Lett. B **716**, 30 (2012) [arXiv:1207.7235 [hep-ex]].
 - [2] G. Aad *et al.* [ATLAS Collaboration], Phys. Lett. B **716**, 1 (2012) [arXiv:1207.7214 [hep-ex]].
 - [3] V. Khachatryan *et al.* [CMS Collaboration], Phys. Lett. B **749**, 337 (2015) [arXiv:1502.07400 [hep-ex]].
 - [4] G. Aad *et al.* [ATLAS Collaboration], JHEP **1511**, 211 (2015) [arXiv:1508.03372 [hep-ex]].
 - [5] M. D. Campos, A. E. C. Hernandez, H. Pas and E. Schumacher, Phys. Rev. D **91**, no. 11, 116011 (2015) [arXiv:1408.1652 [hep-ph]].

- [6] D. Aristizabal Sierra and A. Vicente, Phys. Rev. D **90**, no. 11, 115004 (2014) [arXiv:1409.7690 [hep-ph]].
- [7] C. J. Lee and J. Tandean, JHEP **1504**, 174 (2015) [arXiv:1410.6803 [hep-ph]].
- [8] J. Heeck, M. Holthausen, W. Rodejohann and Y. Shimizu, Nucl. Phys. B **896**, 281 (2015) [arXiv:1412.3671 [hep-ph]].
- [9] A. Crivellin, G. D'Ambrosio and J. Heeck, Phys. Rev. Lett. **114**, 151801 (2015) [arXiv:1501.00993 [hep-ph]].
- [10] I. Dorsner, S. Fajfer, A. Greljo, J. F. Kamenik, N. Kosnik and I. Nisandzic, JHEP **1506**, 108 (2015) [arXiv:1502.07784 [hep-ph]].
- [11] Y. Omura, E. Senaha and K. Tobe, JHEP **1505**, 028 (2015) [arXiv:1502.07824 [hep-ph]].
- [12] A. Crivellin, G. D'Ambrosio and J. Heeck, Phys. Rev. D **91**, no. 7, 075006 (2015) [arXiv:1503.03477 [hep-ph]].
- [13] D. Das and A. Kundu, Phys. Rev. D **92**, no. 1, 015009 (2015) [arXiv:1504.01125 [hep-ph]].
- [14] F. Bishara, J. Brod, P. Uttayarat and J. Zupan, JHEP **1601**, 010 (2016) [arXiv:1504.04022 [hep-ph]].
- [15] I. de Medeiros Varzielas, O. Fischer and V. Maurer, JHEP **1508**, 080 (2015) [arXiv:1504.03955 [hep-ph]].
- [16] X. G. He, J. Tandean and Y. J. Zheng, JHEP **1509**, 093 (2015) [arXiv:1507.02673 [hep-ph]].
- [17] C. W. Chiang, H. Fukuda, M. Takeuchi and T. T. Yanagida, JHEP **1511**, 057 (2015) [arXiv:1507.04354 [hep-ph]].
- [18] W. Altmannshofer, S. Gori, A. L. Kagan, L. Silvestrini and J. Zupan, Phys. Rev. D **93**, no. 3, 031301 (2016) [arXiv:1507.07927 [hep-ph]].
- [19] K. Cheung, W. Y. Keung and P. Y. Tseng, Phys. Rev. D **93**, no. 1, 015010 (2016) [arXiv:1508.01897 [hep-ph]].
- [20] E. Arganda, M. J. Herrero, X. Marcano and C. Weiland, Phys. Rev. D **93**, no. 5, 055010 (2016) [arXiv:1508.04623 [hep-ph]].
- [21] F. J. Botella, G. C. Branco, M. Nebot and M. N. Rebelo, Eur. Phys. J. C **76**, no. 3, 161 (2016) [arXiv:1508.05101 [hep-ph]].
- [22] S. Baek and K. Nishiwaki, Phys. Rev. D **93**, no. 1, 015002 (2016) [arXiv:1509.07410 [hep-ph]].
- [23] W. Huang and Y. L. Tang, Phys. Rev. D **92**, 094015 (2015) [arXiv:1509.08599 [hep-ph]].
- [24] S. Baek and Z. F. Kang, JHEP **1603**, 106 (2016) [arXiv:1510.00100 [hep-ph]].

- [25] E. Arganda, M. J. Herrero, R. Morales and A. Szynekman, JHEP **1603**, 055 (2016) [arXiv:1510.04685 [hep-ph]].
- [26] D. Aloni, Y. Nir and E. Stamou, arXiv:1511.00979 [hep-ph].
- [27] R. Benbrik, C. H. Chen and T. Nomura, arXiv:1511.08544 [hep-ph].
- [28] Y. Omura, E. Senaha and K. Tobe, arXiv:1511.08880 [hep-ph].
- [29] H. B. Zhang, T. F. Feng, S. M. Zhao, Y. L. Yan and F. Sun, arXiv:1511.08979 [hep-ph].
- [30] L. T. Hue, H. N. Long, T. T. Thuc and N. T. Phong, arXiv:1512.03266 [hep-ph].
- [31] N. Bizot, S. Davidson, M. Frigerio and J.-L. Kneur, JHEP **1603**, 073 (2016) [arXiv:1512.08508 [hep-ph]].
- [32] X. F. Han, L. Wang and J. M. Yang, arXiv:1601.04954 [hep-ph].
- [33] C. F. Chang, C. H. V. Chang, C. S. Nugroho and T. C. Yuan, arXiv:1602.00680 [hep-ph].
- [34] C. H. Chen and T. Nomura, arXiv:1602.07519 [hep-ph].
- [35] C. Alvarado, R. M. Capdevilla, A. Delgado and A. Martin, arXiv:1602.08506 [hep-ph].
- [36] S. Banerjee, B. Bhattacharjee, M. Mitra and M. Spannowsky, arXiv:1603.05952 [hep-ph].
- [37] A. Hayreter, X. G. He and G. Valencia, arXiv:1603.06326 [hep-ph].
- [38] K. Huitu, V. Keus, N. Koivunen and O. Lebedev, arXiv:1603.06614 [hep-ph].
- [39] I. Chakraborty, A. Datta and A. Kundu, arXiv:1603.06681 [hep-ph].
- [40] A. Lami and P. Roig, arXiv:1603.09663 [hep-ph].
- [41] T. T. Thuc, L. T. Hue, H. N. Long and T. P. Nguyen, arXiv:1604.03285 [hep-ph].
- [42] E. Arganda, A. M. Curiel, M. J. Herrero and D. Temes, Phys. Rev. D **71**, 035011 (2005) [hep-ph/0407302].
- [43] G. Blankenburg, J. Ellis and G. Isidori, Phys. Lett. B **712**, 386 (2012) [arXiv:1202.5704 [hep-ph]].
- [44] A. Arhrib, Y. Cheng and O. C. W. Kong, Europhys. Lett. **101**, 31003 (2013) [arXiv:1208.4669 [hep-ph]].
- [45] R. Harnik, J. Kopp and J. Zupan, JHEP **1303**, 026 (2013) [arXiv:1209.1397 [hep-ph]].
- [46] A. Dery, A. Efrati, Y. Hochberg and Y. Nir, JHEP **1305**, 039 (2013) [arXiv:1302.3229 [hep-ph]].
- [47] M. Arana-Catania, E. Arganda and M. J. Herrero, JHEP **1309**, 160 (2013) [JHEP **1510**, 192 (2015)] [arXiv:1304.3371 [hep-ph]].
- [48] M. Arroyo, J. L. Diaz-Cruz, E. Diaz and J. A. Orduz-Ducuara, arXiv:1306.2343 [hep-ph].

- [49] A. Celis, V. Cirigliano and E. Passemar, Phys. Rev. D **89**, 013008 (2014) [arXiv:1309.3564 [hep-ph]].
- [50] A. Falkowski, D. M. Straub and A. Vicente, JHEP **1405**, 092 (2014) [arXiv:1312.5329 [hep-ph]].
- [51] E. Arganda, M. J. Herrero, X. Marcano and C. Weiland, Phys. Rev. D **91**, no. 1, 015001 (2015) [arXiv:1405.4300 [hep-ph]].
- [52] A. Dery, A. Efrati, Y. Nir, Y. Soreq and V. Susic, Phys. Rev. D **90**, 115022 (2014) [arXiv:1408.1371 [hep-ph]].
- [53] Seungwon Baek, Takaaki Nomura, and Hiroshi Okada, work in progress.
- [54] J. Adam *et al.* [MEG Collaboration], Phys. Rev. Lett. **110**, 201801 (2013) [arXiv:1303.0754 [hep-ex]].
- [55] K. Griest and D. Seckel, Phys. Rev. D **43**, 3191 (1991).
- [56] J. Edsjo and P. Gondolo, Phys. Rev. D **56**, 1879 (1997) [hep-ph/9704361].
- [57] P. A. R. Ade *et al.* [Planck Collaboration], Astron. Astrophys. (2014) [arXiv:1303.5076 [astro-ph.CO]].
- [58] J. M. Cline, K. Kainulainen, P. Scott and C. Weniger, Phys. Rev. D **88** (2013) 055025 Erratum: [Phys. Rev. D **92** (2015) no.3, 039906] [arXiv:1306.4710 [hep-ph]].
- [59] M. A. Shifman, A. I. Vainshtein and V. I. Zakharov, Phys. Lett. B **78**, 443 (1978).
- [60] G. Belanger, F. Boudjema, A. Pukhov and A. Semenov, Comput. Phys. Commun. **185**, 960 (2014) [arXiv:1305.0237 [hep-ph]].
- [61] D. S. Akerib *et al.* [LUX Collaboration], Phys. Rev. Lett. **112**, 091303 (2014) [arXiv:1310.8214 [astro-ph.CO]].
- [62] G. W. Bennett *et al.* [Muon G-2 Collaboration], Phys. Rev. D **73**, 072003 (2006) [hep-ex/0602035].
- [63] F. Jegerlehner and A. Nyffeler, Phys. Rept. **477**, 1 (2009) [arXiv:0902.3360 [hep-ph]].
- [64] A. Belyaev, N. D. Christensen and A. Pukhov, Comput. Phys. Commun. **184**, 1729 (2013) [arXiv:1207.6082 [hep-ph]].
- [65] P. M. Nadolsky, H. L. Lai, Q. H. Cao, J. Huston, J. Pumplin, D. Stump, W. K. Tung and C.-P. Yuan, Phys. Rev. D **78**, 013004 (2008) [arXiv:0802.0007 [hep-ph]].
- [66] C. Arina, R. N. Mohapatra and N. Sahu, Phys. Lett. B **720**, 130 (2013) [arXiv:1211.0435 [hep-ph]].